Simulation and Hardware Implementation of New Maximum Power Point Tracking Technique for Partially Shaded PV System Using Hybrid DEPSO Method

Mohammadmehdi Seyedmahmoudian, *Member, IEEE*, Rasoul Rahmani, *Member, IEEE*, Saad Mekhilef, *Senior Member, IEEE*, Amanullah Maung Than Oo, Alex Stojcevski, Tey Kok Soon, and Alireza Safdari Ghandhari

***Abstract*—In photovoltaic (PV) power generation, partial shading is an unavoidable complication that significantly reduces the efficiency of the overall system. Under this condition, the PV system produces a multiple-peak function in its output power characteristic. Thus, a reliable technique is required to track the global maximum power point (GMPP) within an appropriate time. This study aims to employ a hybrid evolutionary algorithm called the DEPSO technique, a combination of the differential evolutionary (DE) algorithm and particle swarm optimization (PSO), to detect the maximum power point under partial shading conditions. The paper starts with a brief description about the behavior of PV systems under partial shading conditions. Then, the DEPSO technique along with its implementation in maximum power point tracking (MPPT) is explained in detail. Finally, Simulation and experimental results are presented to verify the performance of the proposed technique under different partial shading conditions. Results prove the advantages of the proposed method, such as its reliability, system-independence, and accuracy in tracking the GMPP under partial shading conditions.**

***Index Terms*—Differential evolution (DE) algorithm, maximum power point tracking (MPPT), partial shading, particle swarm optimization (PSO), photovoltaic (PV) system.**

I. Introduction

PHOTOVOLTAIC (PV) systems possess several fundamental advantages compared with other means of harvesting renewable energy [1]. The main advantages of PV systems include the following: 1) static, quiet, and movement-free characteristics; 2) longevity; and 3) low-maintenance costs. Using PV modules individually is not recommended because of minimal power yield. To provide the load with the precise voltage and current needed, both series and parallel configurations of PV modules are often employed [2]. By contrast, using bypass diodes on related configurations of PV modules produces partial shading. The detrimental effects of partial shading on PV array efficiency still exist despite advancements in technology. Specifically, partial shading alters the output of the array, thereby resulting in a nonlinear power–voltage (P–V) relationship and multiple-peak characteristics. The latter effect diminishes the efficiency of conventional maximum power point tracking (MPPT) methods [3], [4].

In a PV system, many PV modules are often connected in series and/or parallel to provide a system with the required voltage and feeding current capacity. As a result, partial shading is typically inescapable because some parts of the array or the PV system receive low solar irradiance because of shadows of clouds, trees, buildings, and other neighboring items. Partial shading significantly influences the efficiency of the output of PV systems depending on the system architecture, shading scheme, or even the number of bypass diodes integrated into the PV modules.

The consequence of partial shading conditions on PV systems is extensively studied in literature [5], [6]. Under these conditions, a PV module that belongs to the same string receives different insolation. The output P–V characteristic curve becomes complicated and consequently yields a multiple-peak curve. The emergence of multiple peaks in the output characteristics of PV systems reduces the efficiency of ordinary MPPT methods, assuming that an individual maximum power point (MPP) exists on the P–V characteristic. These techniques are based on "hill-climbing" theory to shift the following operating point in the direction where the output power is optimized. These strategies obtain only a local MPP because the P–V curve is multimodal.

Given that the drawbacks of partial shading are common, an appropriate MPPT technique that can find the global MPP (GMPP) under any mismatching condition should be developed. Some studies have focused on GMPP tracking strategies

Manuscript received October 12, 2014; revised January 27, 2015; accepted February 22, 2015. Date of publication April 16, 2015; date of current version June 17, 2015. This work was supported in part by Deakin University Research and in part by the High Impact Research-Ministry of Higher Education (HIR-MOHE) under project Grant UM.C/HIR/MOHE/ENG/24. Paper no. TSTE-00573-2014.

M. Seyedmahmoudian, A. Maung Than Oo, and A. Stocevski are with the School of Engineering, Faculty of Science, Engineering and Built Environment, Deakin University, Geelong 3216, Australia (e-mail: mseyedma@deakin.edu.au; aman.m@deakin.edu.au; alex.stojcevski@deakin.edu.au).

R. Rahmani is with the Centre for Artificial Intelligence and Robotics, Universiti Teknologi Malaysia, Kuala Lumpur 54100, Malaysia (e-mail: r.r.rahmani@ieee.org).

S. Mekhilef, T. K. Soon, and A. S. Ghandhari are with the Power Electronics and Renewable Energy Research Laboratory (PEARL), Department of Electrical Engineering, University of Malaya, Kuala Lumpur 50603, Malaysia (e-mail: Saad@um.edu.my).

Color versions of one or more of the figures in this paper are available online at http://ieeexplore.ieee.org.

Digital Object Identifier 10.1109/TSTE.2015.2413359

under nonuniform irradiance levels [7]–[21]. In [7], a double-stage technique for GMPP tracking is discussed. The procedure for this method is based on recognizing the neighboring areas of the MPP in the first stage and on tracking the actual GMPP in the second stage. However, this method cannot track the actual GMPP in all partial shading conditions, particularly when the load intersecting the output curve is on the right side of the GMPP. A new MPPT approach that works under partial shading conditions is introduced in [8]. In this method, the voltage values of each MPP must be previously evaluated. Therefore, the proposed technique becomes system-dependent. The authors in [9] and [10] proposed a Fibonacci-based technique to track the GMPP. In a procedure similar to the perturbation and observation (P&O) method, the measured power of two points determines the movement of the next operating point. The difference between this technique and the P&O method is the use of the Fibonacci sequence to determine the step size; this approach enhances the tracking speed. However, the drawback of the conventional P&O method still remains; therefore, tracking the GMPP, under all partial shading conditions, is not guaranteed. In [11], another double-stage scheme is proposed to find the actual GMPP under a crucial partial shading condition. In the first stage, all the local MPPs are monitored; the GMPP is then tracked by using the P&O method in the second stage. Although the method has a comparably high efficiency, the drawback is that the algorithm is required to scan almost all ranges of the search space in some partial shading conditions. Therefore, tracking the GMPP takes a long process with this method. In another two-stage method, the dividing rectangle search method is employed to find the region of the GMPP. Once the stopping condition is met, the exact GMPP is tracked by using the P&O method. The output result presented in the article proves the reliability of the method in certain partial shading conditions. However, this method is complex and thus considerably increases the computation cost of the system. In [12], a method called "extremum seeking control" is tested under different partial shading conditions. This method models the PV array characteristic in its tracking process on the basis of the segmental search concept. The technique is quite efficient in finding the GMPP; however, this method has system dependency and produces initial steady-state errors.

Artificial intelligence techniques, such as fuzzy logic control (FLC) and artificial neural network (ANN) methods, have been popular among researchers [22]–[25]. The authors in [22] propose the efficient and reliable FLC method to track the MPP under partial shading conditions. In [23], the fuzzy logic controller is used to enhance the performance of Hill-climbing method, by scanning and storing the MPP during the perturbing and observing procedures. In [24], the FLC with ANN is employed to track the GMPP. In this method, the irradiance level and cell temperature are the main inputs to train the ANN process to find the MPP. The mentioned proposed methods have shown the satisfactory performance for finding the GMPP, under normal and certain partial shading conditions. However, these methods need extensive computation in the fuzzification, rule base, and defuzzification stages.

The particle swarm optimization (PSO) technique has also been proposed in several publications [26]–[29]. The metaheuristic approach of this method makes it independent of the output characteristics of PV systems. Miyataki [26] and Liu [27] comprehensively investigated the global tracking of the actual MPP in a modular configuration of the PV system. The authors achieved accurate results even by reducing the number of sensors in their experiment. However, they used standard PSO, which is associated with several drawbacks. In standard PSO, high velocity must be used for a particle whose position is too far from the best particles' position (Gbest), defined as the best experienced position of all particles. In addition, the trajectory of the particles is limited by designed acceleration. Low acceleration results in a smooth trajectory for particles but slow convergence; by contrast, high acceleration may accelerate computation but may lead the particles toward infinity [30]. Random coefficients in the cognitive and social components of the PSO algorithm are significant parameters in optimization. A low-value design for this coefficient may result in slight perturbation movement. Thus, further iteration must be conducted to bring the operating point to an optimum value. A large-design random coefficient increases perturbation and traps the operation point in the search space margins or local MPPs.

In view of these problems, some studies have modified the standard PSO technique [31]–[33]. Chowdhury *et al.* [31] modified the perception radius and search direction of each agent in accordance with its performance improvement throughout algorithm iterations. In this method, which is called "adaptive perceptive PSO (APPSO)" all agents have to scan their own range of search space. This modification significantly increases the accuracy of the algorithm to find the global maximum. However, in this method, the additional dimensional search space leads the designer to assign a higher number of particles. Consequently, this method boosts the computational burden and complexity of implementation. Ishaque *et al.* [33] tracked the global maximum accurately by proposing deterministic PSO (DPSO) method. Experimental results show fast and accurate tracking process in some partial shading conditions. However, given the removed random numbers in this method, the algorithm loses the main advantage of evolutionary algorithms and cannot track the global maximum in all partial shading patterns. In [34], Lian *et al.* employed P&O to improve the convergence speed of PSO. In the proposed method, the P&O identifies the nearest local MPPs in the first step and then the PSO starts searching the GMPP in the second step. As a result of using this combination, the search space exploration is reduced in early iterations.

This study is conducted to set a robust, fast, and efficient global MPPT technique for PV systems under different partial shading conditions. In accordance with literature, some researchers have successfully evaluated the pros and cons of standard PSO under these conditions. Several experts then modified the typical PSO technique to mitigate the drawbacks of the previous concept. However, the advantages of standard PSO are somehow diminished in some of the modified forms. In this paper, the authors use a hybrid evolutionary algorithm called DEPSO, a combination of differential evolution (DE) and PSO, both of which are swarm-based techniques, to track the GMPP under different partial shading conditions. Using DEPSO in GMPP tracking systems provides several advantages. 1) As a

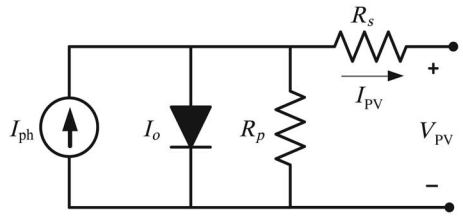

Fig. 1. Equivalent circuit of the PV cell.

result of the stochastic nature of both algorithms, the system is purely independent of the output shape of the PV array. 2) Given the random values in the algorithm architecture, the metaheuristic approach of evolutionary algorithms is not avoided. 3) In contrast to the other modified forms of PSO, the algorithm continues to search the GMPP until a justifiable stopping condition is met. 4) Given the simple approach of the proposed hybrid technique, the computational burden of the algorithm is reduced; thus, the system can be experimentally implemented by using a low-cost microcontroller.

The authors conducted a comprehensive study by describing the appearance of the partial shading and by proposing an effective solution to track the MPP during these conditions. Section I presents the details about the causes and effects of partial shading conditions. A brief introduction of the DE and PSO methods is followed by a description of the implementation of the proposed DEPSO method in the MPP tracking system. Thereafter, the performance of the proposed method is tested under different partial shading conditions by using MATLAB–Simulink software. Finally, the experimental results of the DEPSO method applied to an actual PV system are described.

II. PV System Modeling

Fig. 1 presents a single-diode circuitry for a PV cell. The output of PV systems is directly affected by solar irradiance and temperature. Thus, to obtain the MPP, the latest values of these factors should be employed. Furthermore, the mathematical model of PV changes with the short-circuit current ($I_{\rm sc}$) and the open-circuit voltage ($V_{\rm oc}$), which are obtained from the data sheet provided by the cell manufacturer.

In this context, the generated power of a single solar cell is inadequate for any convenient application. Thus, the cells in the PV system should be connected either in series or in parallel to enhance the overall capability of the system. Therefore, all cells in the PV module (N_s being the given number) contribute to the output power. The module output current can be obtained by using the following equation:

$$I_{{\rm PV}a} = I_{\rm ph} - I_{o1} \times \left[\exp\left(\frac{q(V_{\rm PV}+I_{\rm PV}R_s)}{N_sAKT_k}\right)-1\right] - \frac{(V_{\rm PV}+I_{\rm PV}R_sN_s)}{R_pN_s} = 0 \quad (1)$$

where $I_{\rm PV}$ and $V_{\rm PV}$ refer to the output current and output voltage, respectively. $I_{\rm PV}$ and $V_{\rm PV}$ will be added through the load or network grid. I_{o1} refers to the diode saturation, A stands for the diode ideality factor, q is the electron charge

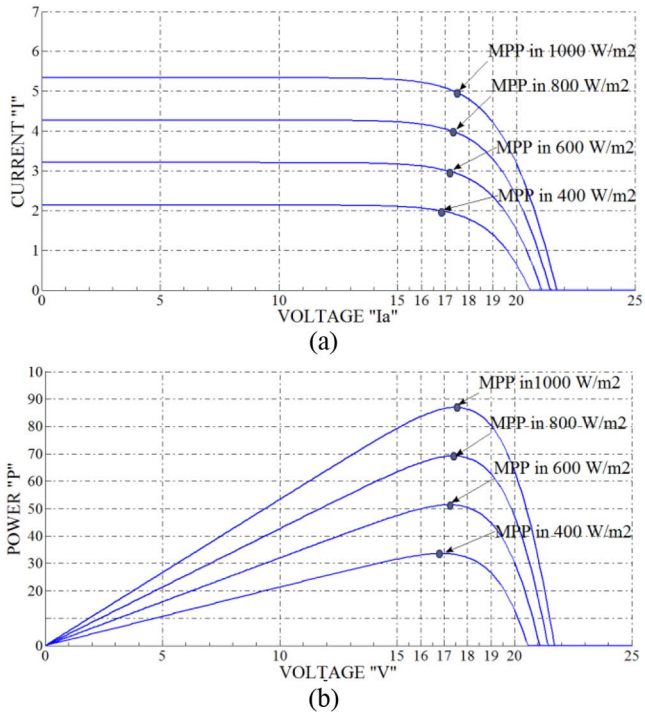

Fig. 2. Output characteristics of PV module under normal conditions: (a) I–V characteristic and (b) P–V characteristic.

TABLE I
KC85T PV Module Specifications

Electrical characteristics	KC85T
Open circuit voltage	21.7 V
Short circuit current	5.34 A
Maximum power voltage	17.4 V
Maximum power current	5.02 A
Maximum power	87 W
Temperature coefficient of $I_{\rm SC}$	2.12×10^{-3} A/°C
Temperature coefficient of $V_{\rm OC}$	-8.21×10^{-2} V/°C

constant ($q = 1.602 \times 10^{-19}$ C), K represents the Boltzmann constant, T_k is the operating temperature that is equal to the reference temperature (25°C) in this paper, and $I_{\rm ph}$ represents the solar-generated current, which can be defined by

$$I_{\rm ph} = (I_{\rm scr})\frac{G}{G_r}. \quad (2)$$

In (1), the parallel resistance (R_p) generally has a high value and sometimes assumes infinity in PV module modeling because of its slight impression. By contrast, the value of series resistance (R_S) cannot be neglected because of its effect on output power. Fig. 2 depicts the output of the KC85T PV module under different irradiance levels. Table I provides detailed information on the electrical parameters.

A. Characteristics of the PV System Under Partial Shading

The entire PV system or some of its parts may be shaded by passing clouds, trees, and high buildings in outdoor

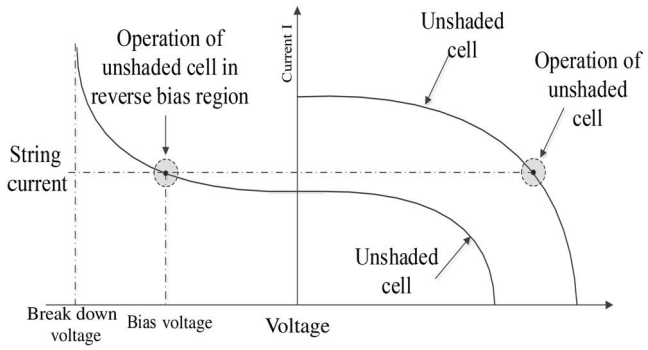

Fig. 3. I–V characteristic of PV cell in reverse-biased region.

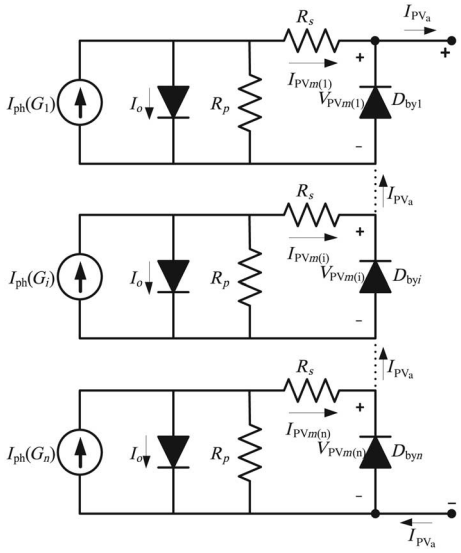

Fig. 4. Circuit model of array consisting of k series-connected array.

environments. This scenario results in nonuniform insolation conditions. A fraction of the PV modules that receive uniform irradiance keeps operating at optimum efficiency during partial shading. Fig. 3 shows that the shaded cells operate with a reverse bias voltage to provide the same current as the unshaded cells because of the constant current flow through every module in a series configuration. However, the resulting reverse power polarity consumes power and reduces the maximum output power of the partially shaded PV module. Exposing the shaded cells to an excessive reverse bias voltage can result in the appearance of "hotspots" and the creation of an open circuit in the entire PV module. This phenomenon is usually solved by inserting a bypass diode to a predefined number of cells in the series circuit.

Fig. 4 shows k series-connected PV modules with allocated bypass diodes in the array. The characteristics of a PV system with bypass diodes are different from those without such diodes. Given that bypass diodes provide an alternate current path, the cells of a module do not have the same current in partial shading conditions. Therefore, the P–V curve creates multiple maxima. Fig. 5 shows the differences of extractable MPP in the PV array with and without bypass diodes. However, the presence of multiple maxima in the P–V curve is an important issue, and most common MPPT techniques cannot determine the difference between local and global maxima.

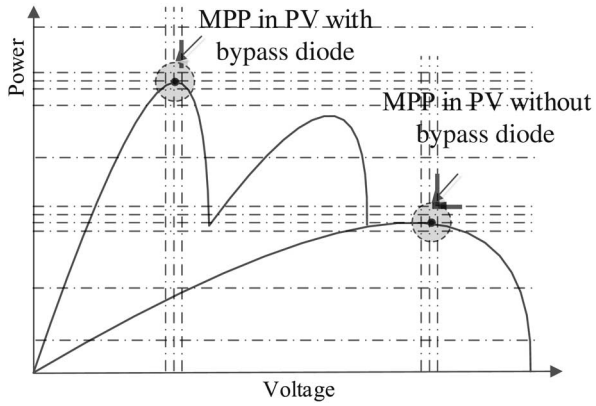

Fig. 5. P–V curve of PV array under partial shading conditions.

The bypass diode restricts the reverse voltage to less than the breakdown voltage of the PV cells if the generated current ($I_{\rm ph}$) of the ith module is reduced to less than the current generated by the entire array. Therefore, the ith bypass diode shown in Fig. 4 operates only when (3) is satisfied. On the basis of the measured solar-generated current of the PV module, these diodes can be mathematically modeled as one resistance. Equation (4) shows that a bypass diode is represented as high resistance ($10^{10}\ \Omega$) when it is reverse-biased and as low resistance ($10^{-2}\ \Omega$) when it is forward-biased [35]

$$I_{{\rm PV}a} > I_{{\rm ph}(i)} \tag{3}$$

$$R_{\rm by}(I_{\rm ph}) = \begin{cases} 10^{-2} D_{\rm by ON} \\ 10^{10} D_{\rm by OFF} \end{cases}. \tag{4}$$

The number of bypass diodes allocated for each module changes depending on the usage requirements and manufacturer purposes. In the modeling and simulation stages, the module with more than one bypass diode can be divided into several submodules with one bypass diode. For instance, a module with two bypass diodes can be considered two submodules. Each submodule behaves as one smaller module during the modeling procedure.

B. Partially Shaded Submodule

A partially shaded submodule can be modeled by using two groups of series-connected PV cells connected inside the submodule. Each group receives various levels of irradiance.

Fig. 6 shows the circuit model for a partially shaded submodule, given that no bypass diode is assumed for the cells inside a submodule. The submodule consists of r series-connected cells, wherein s shaded cells receive irradiance *G1* and $(r-s)$ shaded cells receive irradiance *G2*. Equation (5) presents the PV parameters, and (6) presents the output current and voltage. Subscripts 1 and 2 refer to the cell parameter receiving the irradiance of *G1* and *G2*, respectively,

$$\begin{aligned} &I_{\rm ph1} = I_{\rm ph}(G_1), \quad I_{\rm ph2} = I_{\rm ph}(G_2), \\ &N_{S1} = sN_{S1}, \quad N_{S2} = (r-s)N_{S2} \end{aligned} \tag{5}$$

$$\begin{aligned} I_{{\rm PV}m} &= {\rm Min}(I_{\rm PV1}, I_{\rm PV2}) \\ V_{{\rm PV}m} &= \sum V_{{\rm PV}(i).} \end{aligned} \tag{6}$$

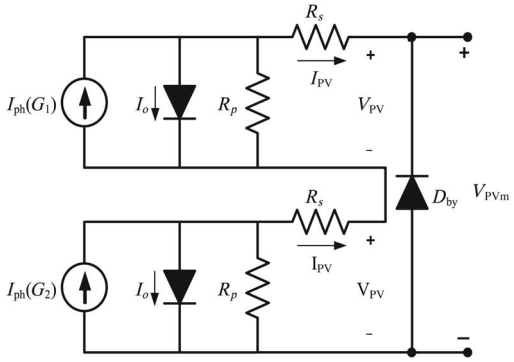

Fig. 6. Circuit diagram of partially shaded submodule.

C. Partially Shaded Array

In the experiment, solar arrays with several PV modules are used to generate a high level of electrical output power. The output power of the array may lead to a complicated form under a partial shading situation. This section mathematically analyzes the output characteristics of the PV array comprising several modules in an array (or PV module comprising several submodules connected to the bypass diodes) [36]. Assuming that two bypass diodes are present for each PV module, to find the output characteristics of the array, the following steps should be considered:

1) determine the solar irradiance received by each module and determine the irradiance matrix;
2) calculate the $I_{\rm ph}$ and Ns of each module by using (5) and define the $I_{\rm ph}$ and Ns matrixes with respect to their solar irradiances;
3) rearrange the $I_{\rm ph}$ matrix from the highest value to the lowest value;
4) compute the output current of array ($I_{{\rm PV}a}$) by using (7), as shown at the bottom of the page, where $I_{{\rm PV}m(i)}$ is the output current of the ith module;
5) determine the output PV voltage ($V_{{\rm PV}a}$) according to (8), as shown at the bottom of the page, where $V_{{\rm PV}m(i)}$ is the output voltage of the ith module.

III. Particle Swarm Optimization

A. Overview of PSO Algorithm

PSO is a swarm-based evolutionary algorithm that investigates the search space and determines the components and settings required to optimize a special objective function [37]. The operation begins with a random selection, continues with a search for optimal solutions through earlier iterations, and evaluates the quality of the solutions through their fitness. The PSO algorithm is a suitable technique for deriving the global optimum. This algorithm is also simple in principle and has high tracing accuracy and a good convergence profile.

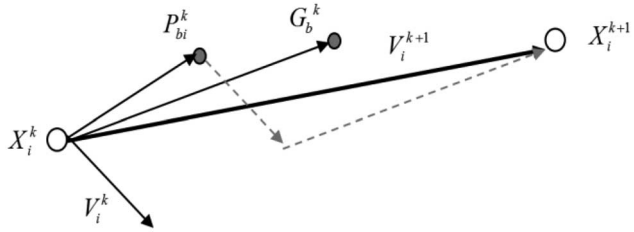

Fig. 7. Simple vector diagram of the motion path of a particle in PSO algorithm.

The PSO algorithm hires a certain number of particles (N) to explore the D-dimensional search space of the problem. At each iteration, every single particle represents a solution to the problem on the basis of the particle's location in the search space Xi. The particles move stochastically using a velocity vector of $\boldsymbol{V}_i$, a resultant of three vectors: 1) the best location experienced by the particle ($P_{\rm bi}$); 2) the best location experienced by the entire swarm (G_b); and 3) a portion of itself in the last iteration. Fig. 7 shows a simple representation of the movement of a particle in the search space.

$P_{\rm bi}$ and G_b must be updated at each iteration throughout the optimization process. To do so, a fitness function should be defined to evaluate the location of each particle at each step. The mathematical form of obtaining the velocity and updating the location of each particle is shown in (9) and (10), respectively,

$$\begin{aligned}\boldsymbol{V}_i^{k+1} = w \times \boldsymbol{V}_i^k + r_1 \times c_1 \times \left(P_{\rm bi} - \boldsymbol{X}_i{}^k\right) \\ + r_2 \times c_2 \times \left(G_b - \boldsymbol{X}_i{}^k\right)\end{aligned} \tag{9}$$

$$\boldsymbol{X}_i{}^{k+1} = \boldsymbol{X}_i{}^k + \boldsymbol{V}_i^k. \tag{10}$$

Here, the subscript i represents the particle number; k denotes the iteration number; $\boldsymbol{V}_i^k$ and $\boldsymbol{X}_i^k$ are the velocity vector and location of the ith particle, respectively, at the kth iteration; r_1 and r_2 are random values chosen from a uniform distribution from 0 to 1; c_1 and c_2 are the cognitive ands

$$I_{{\rm PV}a} = \begin{cases} I_{\rm ph}\left(G_n\right) - I_{o1}\left[\exp\left(\dfrac{q(V_{{\rm PV}mn} + I_{\rm PV}R_s)}{N_s AKT_k}\right) - 1\right] - \dfrac{(V_{{\rm PV}mn} + I_{\rm PV}R_sN_s)}{R_pN_s}, & I_{{\rm PV}a} > I_{{\rm ph}n-1} \\ I_{\rm ph}\left(G_{n-1}\right) - I_{o1}\left[\exp\left(\dfrac{q(V_{{\rm PV}mn-1} + I_{\rm PV}R_s)}{N_s AKT_k}\right) - 1\right] - \dfrac{(V_{{\rm PV}mn-1} + I_{\rm PV}R_sN_s)}{R_pN_s}, & I_{{\rm ph}n-2} < I_{{\rm PV}a} < I_{{\rm ph}n-1} \\ I_{\rm ph}\left(G_1\right) - I_{o1}\left[\exp\left(\dfrac{q(V_{{\rm PV}m1} + I_{\rm PV}R_s)}{N_s AKT_k}\right) - 1\right] - \dfrac{(V_{{\rm PV}m1} + I_{\rm PV}R_sN_s)}{R_pN_s}, & I_{{\rm PV}a} < I_{\rm ph1} \end{cases} \tag{7}$$

$$V_{{\rm PV}n} = \begin{cases} V_{{\rm PV}n} & I_{{\rm PV}a} > I_{{\rm ph}n-1} \\ V_{{\rm PV}n} + V_{{\rm PV}n-1} & I_{{\rm ph}n-2} < I_{{\rm PV}a} < I_{{\rm ph}n-1} \\ V_{{\rm PV}n} + V_{{\rm PV}n-1} + \cdots + V_{\rm PV1} & I_{{\rm PV}a} < I_{\rm ph1} \end{cases}. \tag{8}$$

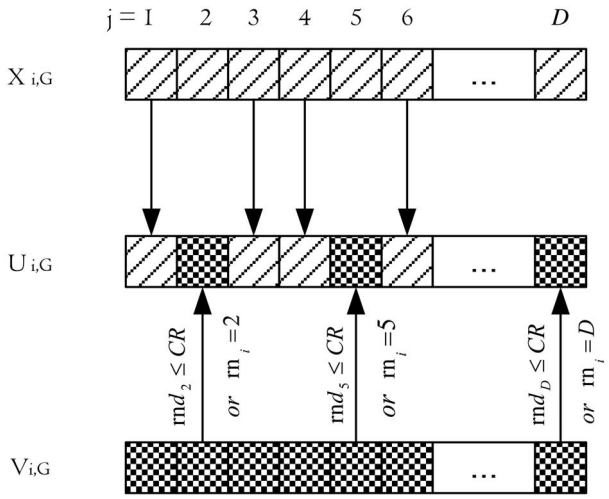

Fig. 8. Generation of the trial vector using target and mutant vectors.

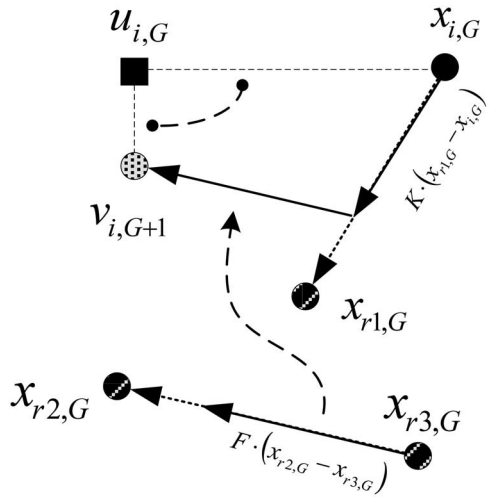

Fig. 9. Process of obtaining a new trial vector in the DE algorithm for a 2-D search space.

social coefficients, respectively; and w is the inertia weight, which decreases continuously throughout the optimization and controls the scale of particle movements.

B. Overview of DE Algorithm

The DE algorithm is a particle-based global optimization algorithm consisting of three main operation sections, namely mutation, crossover, and selection [38]. Equation (11) shows the mutation unit of the DE algorithm, which works as a search engine

$$\boldsymbol{v}_{i,G+1} = \boldsymbol{x}_{i,G} + K \cdot (\boldsymbol{x}_{r1,G} - \boldsymbol{x}_{i,G}) + F \cdot (\boldsymbol{x}_{r2,G} - \boldsymbol{x}_{r3,G}) . \tag{11}$$

Here, $\boldsymbol{v}_{i,G}$ is the mutant vector and $\boldsymbol{x}_{i,G}$ is the target vector of the ith particle at the Gth step. $r_1, r_2,$ and r_3 are random numbers in the range of $1, 2, \ldots \mathrm{nop}$, where nop denotes the number of particles. K and F are the scaling and combination factors, respectively. The crossover or recombination in the DE technique is a nonuniform operation that generates trial vectors on the basis of components from the population. The DE algorithm uses a nonuniform crossover operation to generate trial vectors on the basis of the components of the population. The crossover enables the algorithm to propose better solutions by shuffling the data of the successful combinations. $\boldsymbol{u}_{i,G}$ is the trial vector which is generated based on the two other vectors, namely target vector ($\boldsymbol{x}_{i,G}$) and mutant vector ($\boldsymbol{v}_{i,G}$). The target vector is indeed used for the selection step, which is the last step in the algorithm. To be exact, the new target vector ($\boldsymbol{x}_{i,G+1}$) takes its members based on comparing the fitness values for the old target vector ($\boldsymbol{x}_{i,G}$) and the trial vector ($\boldsymbol{u}_{i,G}$). Equation (12) shows the trial vector of the crossover and Fig. 8 describes how the trial vector is generated using target and mutant vectors

$$\boldsymbol{u}_{i,G} = \begin{cases} \boldsymbol{v}_{i,G}, & \text{if } (\mathrm{rnd}_j \leq \mathrm{CR}) \text{ or } j = \mathrm{rn}_i \\ \boldsymbol{x}_{i,G}, & \text{if } (\mathrm{rnd}_j > \mathrm{CR}) \text{ or } j \neq \mathrm{rn}_i \end{cases} \boldsymbol{Z}. \tag{12}$$

Here, $j \in 1, 2, \ldots, D$, CR is the crossover constant between 0 and 1, rnd_j is a random value between 0 and 1, and rn_i is a random number chosen from the domain of j. The maximum dimension of the search space is denoted by D. Fig. 9 shows the process of obtaining a new trial vector in the DE algorithm for a two-dimensional (2-D) search space.

The final operation is the selection operation that directs the movement toward prospective areas in the search. The selection of the parents is independent of the fitness values; however, the produced children (offspring) in the mutation and crossover must be evaluated by the fitness function and compared with the parents. The parents stay in the population if the fitness values have no effect on the selection of parents. The children produced in the mutation and crossover are then evaluated and compared with the parents. The parents remain in the population if they have better fitness values than their children. The selection procedure can be expressed as follows:

$$\boldsymbol{x}_{i,G+1} = \begin{cases} \boldsymbol{u}_{i,G}, & \text{if } (f(\boldsymbol{x}_{i,G}) \leq f(\boldsymbol{u}_{i,G})) \\ \boldsymbol{x}_{i,G}, & \text{otherwise.} \end{cases} \tag{13}$$

C. DEPSO Algorithm

In the PSO algorithm, as the iteration goes on, the diversity of particles decreases significantly [39]. This phenomenon increases the probability of being trapped in the local optima of the solution space. By contrast, the DE algorithm successfully explores the local optima of the search space by utilizing the differential information; however, this algorithm degrades its search quality in finding the global optima [40]. The DEPSO algorithm keeps individuals from being trapped in the local optima by combining the DE operator with the PSO algorithm, which diversifies the PSO technique [41]. Several applications of training, clustering, and optimization have been presented in literature, which shows that DEPSO outperforms both the PSO and DE algorithms in terms of solution quality and convergence speed [42]. G_b and P_{bi} are important components in the searching process of the PSO algorithm, in which every individual tries to improve its position toward reaching G_b as the best position found by the swarm. However, the decremental weighted velocity of the individuals decreases the ability of the swarm to diversify after a certain iteration. The function of DE in DEPSO is to add diversity to the canonical PSO algorithm and to explore

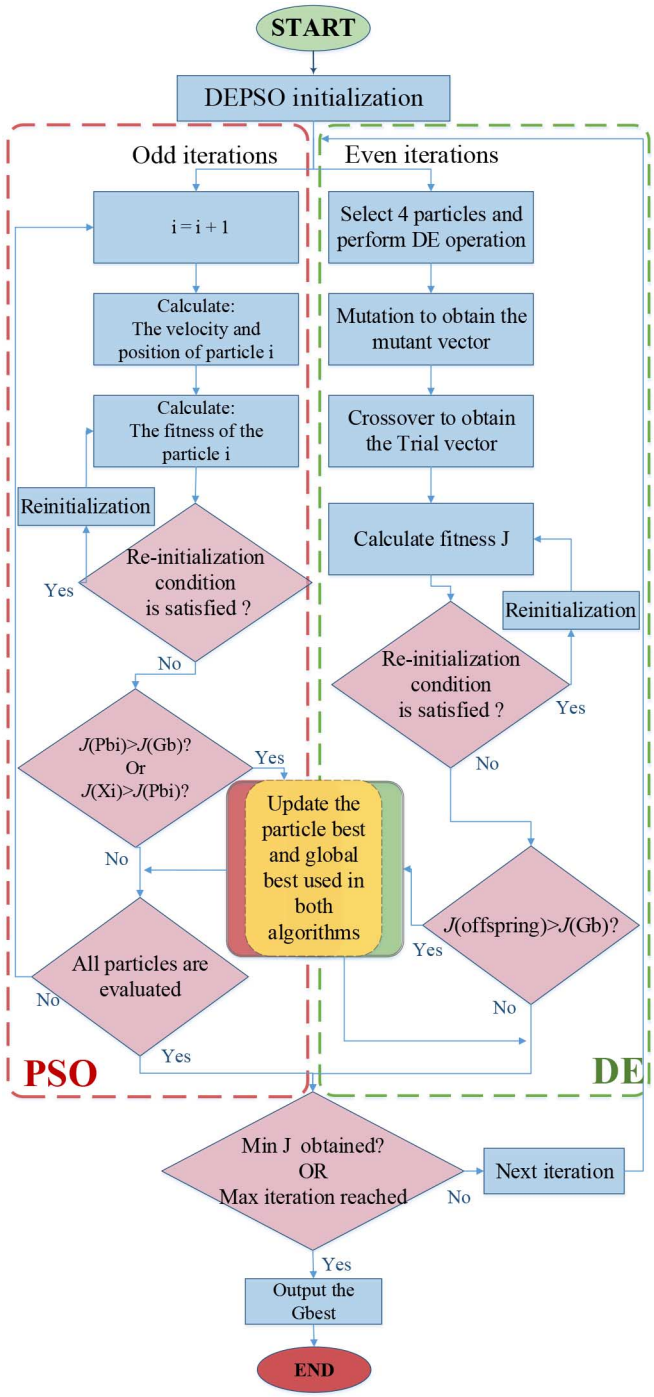

Fig. 10. Flowchart of DEPSO algorithm.

and exploit the search space smartly while the individuals are kept from being stuck to the local optima [41]. Therefore, the PSO algorithm is applied every odd iteration, and the DE mutation operator is implemented in even iterations. Fig. 10 shows a simple flowchart of the process of implementing the DEPSO algorithm, where J represents its fitness function.

D. DEPSO-Based MPPT

The search space of the problem consists of a vector of different values for the terminal voltage of the PV panel.

TABLE II
PARAMETER SELECTION OF THE PROPOSED DEPSO ALGORITHM

$C1$	$C2$	W	CR	F	K
2	1.5	1.2	0.8	0.7	0.5

Equation (14) shows the location vector of the problem, a $1 \times N$ vector, where N denotes the number of particles hired. Each location represents a voltage value that is a potential solution to the MPPT problem. The particles are evaluated based on the output power of the PV panel with respect to the proposed terminal voltage

$$\boldsymbol{X}_i^k = \left[\boldsymbol{X}_1^k,\ \boldsymbol{X}_2^k,\ \ldots,\ \boldsymbol{X}_i^k,\ \ldots,\ \boldsymbol{X}_{N-1}^k,\ \boldsymbol{X}_N^k \right]. \quad (14)$$

In practice, during partial shading, instantaneous variations in the insolation level cause sharp fluctuations in the generated power. Therefore, the condition presented in (15) must be satisfied to initialize the algorithm. The condition indicates the minimum allowed variation in the output power to run the algorithm and to find the new MPP, which is given by ΔP

$$\left| \frac{J(X_{i+1}) - J(X_i)}{J(X_i)} \right| > \Delta P \quad (15)$$

where $J(X_i)$ returns the output power of the PV panel, respective to the location of ith particle in the search space. Given that numerous partial shading conditions can happen and only some of them can be modeled, three controversial conditions are selected in this study to test the proposed MPPT technique. The DEPSO-based MPPT method is tested and analyzed through simulation and experiment. The parameter selection of the DEPSO algorithm is shown in Table II on the basis of successful experiments in literature [42].

IV. SIMULATION

Countless conditions for partial shading can happen. However, to test and describe our proposed technique, three controversial conditions are randomly selected and simulated. Fig. 11 shows the circuitry diagram of the selected PV array, in which two modules are connected in series arrangement. Double-bypass diodes are assumed for each PV module. So, each module can be divided into two submodules. By considering each submodule as a separate module in modeling and simulation process, the three selected partial shading conditions can be described as follows. 1) First condition: the entire module 1 receives irradiance level G1 and the entire module 2 receives irradiance level G2. 2) Second condition: the entire module 1 receives irradiance $G1 = G2$ and module 2 receives different irradiance levels G3 and G4 (submodule 3 receives irradiance G3 and submodule 4 receives irradiance G4). 3) Third condition: partial shading occurs inside both PV modules. Submodules 1 and 2 in module 1 receive irradiance levels G1 and G2, and submodules 3 and 4 in module 2 receive irradiance levels G3 and G4.

A. First Condition

The performance of the proposed technique is tested under the first condition. The first PV module receives an equally

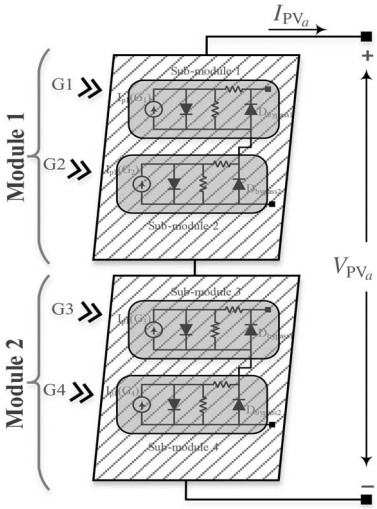

Fig. 11. Circuitry diagram of the selected PV array.

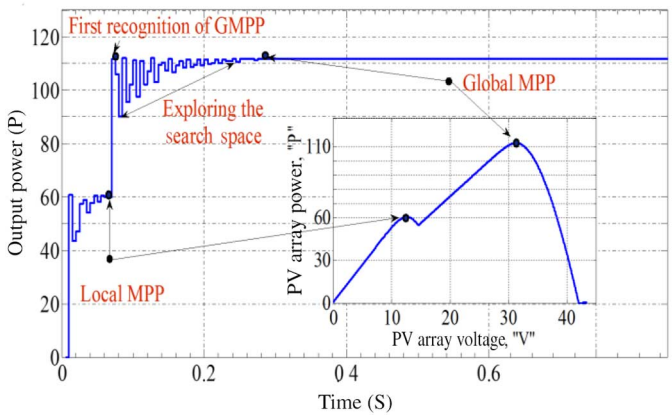

Fig. 12. Simulation results for shading pattern 1.

distributed irradiance level of $G1 = G2$, whereas the second PV module receives $G3 = G4 = 0.7G1$. In this condition, partial shading occurs in the array level, not in the module. Fig. 12 shows the output power characteristics of the PV array along with the simulation results of the proposed method. The presence of the local MPP before the GMPP does not prevent the proposed technique from tracking the correct MPP. The preset conditions for this case exemplify a moderate level of partial shading. Given that there is only single local peak in the output curve and there is a considerable difference in the power of the global and local MPP, the actual MPP can be obtained even by some of the modified conventional techniques. This finding is caused by the fact that some of the conventional methods are modified in the way that they starts the search space from the middle, which attunes them to finding the GMPP under the aforementioned conditions. However, the result of the proposed MPP shows that it evaluates all ranges of search space to find all MPPs, regardless of their location in the search space.

B. Second Condition

For further verification, the system is tested under partial shading conditions in the module level. In this case, the first

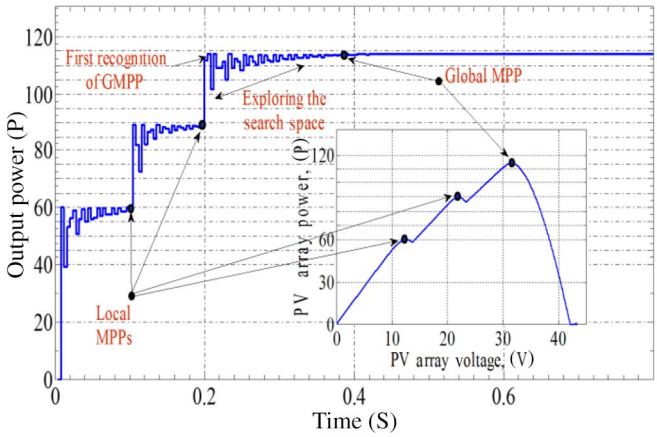

Fig. 13. Simulation results for shading pattern 2.

module receives an equally distributed irradiance level of $G1 = G2$, and the second module receives two irradiance levels of $G3 = 0.9G1$ and $G4 = 0.6G1$. For simplicity, each submodule can be considered as a separate module connected in series inside the array. The second case is similar to the first, but the main difference is that the GMPP occurs after two local MPPs and the difference power value between the global maximum and the nearest local MPP is lower. Most conventional MPPT methods cannot find the actual GMPP in such conditions and are normally trapped in the first MPP, which is not obviously the real GMPP. Thus, the efficiency of the PV systems drops dramatically. Fig. 13 shows the simulation result of the proposed DEPSO technique applied to the second condition. According to the output locus, the local MPPs are initially evaluated and tracked prior to the GMPP. The actual maximum power of the system is found in a comparably short time even after two subsequent local MPPs.

C. Third Condition

This simulation aims to assess the accuracy of the PSO algorithm when the majority of the array falls under a shadow. In this condition, partial shading occurs in both modules; submodules 1 to 4 inside the array receive different irradiance levels of G1, $G2 = 0.6G1$, $G3 = 0.4G1$, and $G4 = 0.2G1$. Of significance are the presenting local maximums before and after the global maximum and the minute difference between the derived GMPP and other corresponding values. Fig. 14 presents the system output power locus and its correlated power characteristic. The simulated power locus proves that the controller accurately tracked the actual MPP, even though the difference between the GMPP and the nearest local MPP is less than 10 W.

V. Experimental Results and Discussions

Fig. 15 shows the experimental configuration and the converters set up of the proposed MPPT technique in our laboratory. The experimental verification is implemented by using an Agilent modular PV simulator (E4360-A series) to create the output characteristic of the PV system. The Atmega328P microcontroller (Atmel Corporation) is used in this research. This

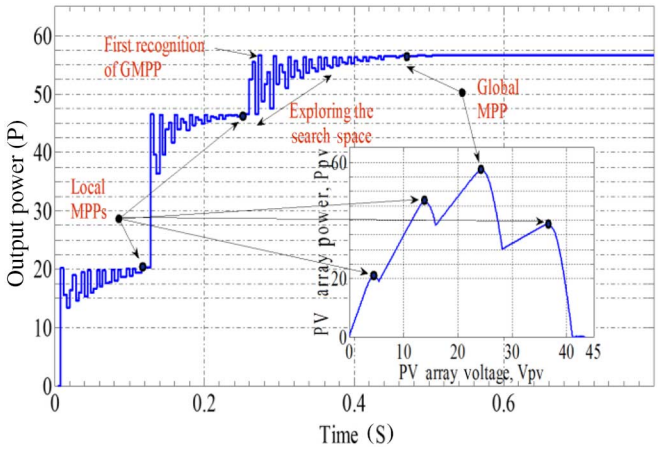

Fig. 14. Simulation results for shading pattern 3.

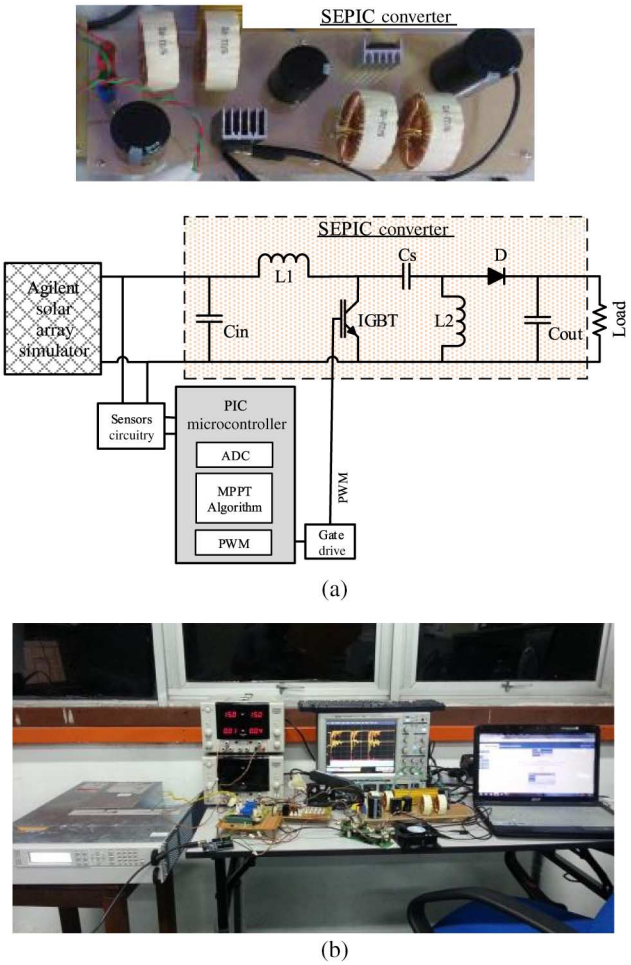

Fig. 15. (a) Block diagram of experimental setup configuration. (b) Test bench photograph.

microcontroller is equipped with 10-bit ADC, which is suitable for this project. A gate drive with a signal frequency of 20 kHz is designed to switch the converter, which regulates the output voltage and tracks the MPP. The dc–dc converter is a buck boost and is a single-ended primary-inductor converter (SEPIC) as shown in Fig. 15(a). The SEPIC converter is able to step up or step down the input voltage similar to the buck-boost converter.

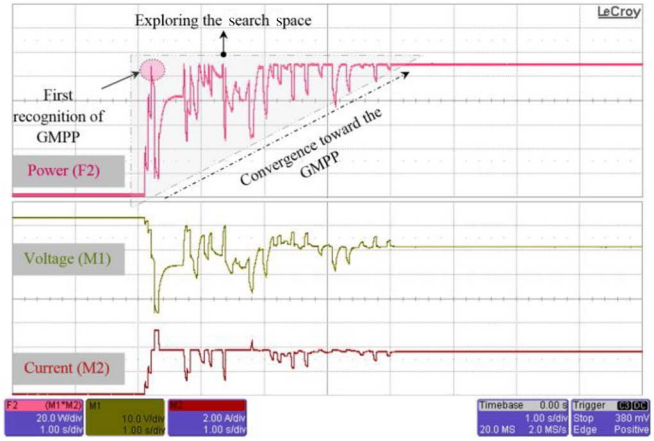

Fig. 16. Output waveforms of shading pattern 1.

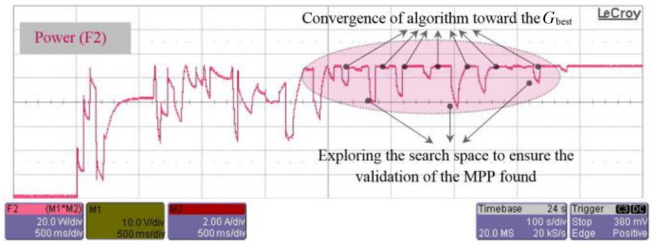

Fig. 17. Zoomed version of Fig. 15.

However, the output voltage of the former is not inverted in contrast to the latter. The SEPIC converter is designed to operate in continuous conduction mode and is chosen on the basis of its wide range of operational region and independency of irradiation, temperature, and output load. Three different schemes of partial shading conditions (Section IV) are uploaded onto the Agilent PV simulator to test experimentally the proposed MPPT method under various weather conditions. The results of these conditions are shown in Figs. 16–20.

Figs. 16 and 17 show the experimental results of the system under condition 1. The entire tracking process takes around 4 s, and the MPP recognition of the GMPP occurs after 0.2 s from the start of the tracking. As a system-independent method, the algorithm has no information about the output waveform of the PV array; thus, the proposed method continues searching until the stopping condition is met even when the GMPP is found in early iterations. As a result, in case of any change in weather conditions or output load, the algorithm considers this change and recognizes it during the running process.

The output locus of the system for condition 2 is shown in Fig. 18, which shows the tracking process of the proposed algorithm and other experimental results. At the initial iteration, a wide range of search space is covered. By contrast, at the final iterations, the algorithm is focused on a narrow range of search space when the possibility of a global maximum is high. This finding is the result of the design of the algorithm parameters described in Section III. D.

To evaluate the system further, condition 3 is uploaded onto the PV simulator to provide the PV curve, in which several local MPPs are presented along with the GMPP. Fig. 19 shows

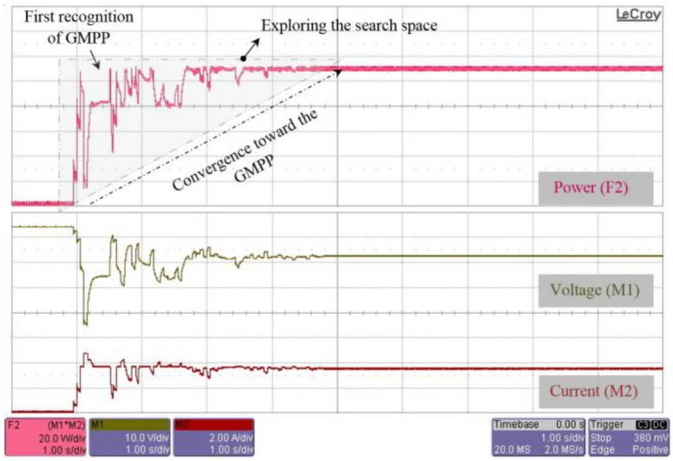

Fig. 18. Output waveforms of shading pattern 2.

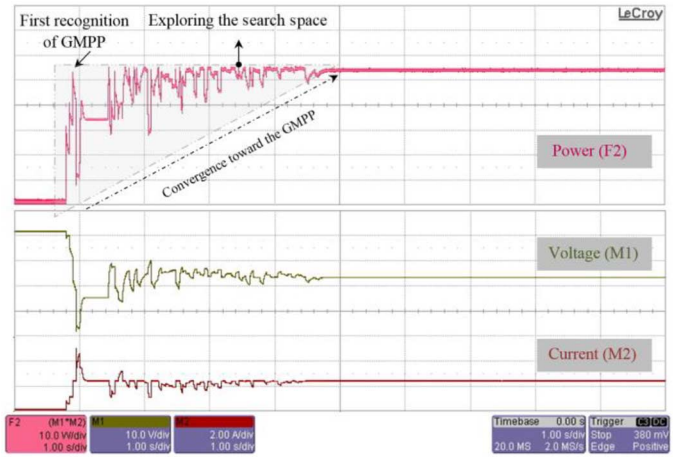

Fig. 19. Output waveforms of shading pattern 3.

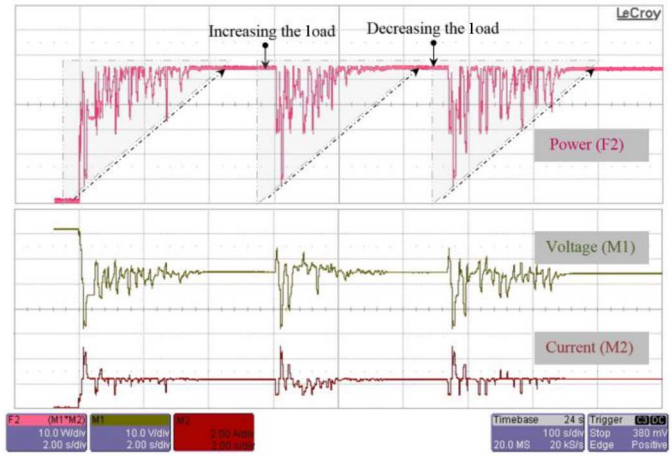

Fig. 20. Output waveforms of shading pattern 3 with changes in load.

that the GMPP is found at $t = 1.4$ s, i.e., at the initial iteration. The algorithm stores this point and continues to find any other possible point in other parts of the search space to ensure that the output result of the algorithm is GMPPs.

In addition to the defined conditions, the proposed algorithm is tested for different load levels when the system is operated in condition 3. Fig. 20 shows that when the controller finds the MPP, the system stabilizes if no change happens. At $t = 6.8$ s, the load is changed to $R = 10$; thus, the controller starts to work. At $t = 10$ s, the MPP stops working by finalizing all iterations and by tracking the MPP. At $t = 12.2$ s, the load is changed to $R = 20$, and the controller starts working until it finds the MPP at $t = 15.8$ s. Changing the output load does not prevent the algorithm from successfully capturing the proper MPP.

TABLE III
OUTPUT RESULTS OF THE DEPSO ALGORITHM UNDER THE THREE CONDITIONS

Test condition	P_A (EXP)	Max. obtained $P_{M\text{MAX}}$ (DEPSO)	Min. obtained $P_{M\text{MIN}}$ (DEPSO)	P_M (DEPSO)	P_{EE} (%)
First condition	111.1	109.8	109	109.2	**98.2**
Second condition	113.1	111.2	109.8	110.5	**98.0**
Third condition	56.1	55.3	54.1	54.6	**97.5**

In accordance to the metaheuristic characteristic of the proposed technique, no information about the output curve is required. Thus, the algorithm is tested around 100 times under different partial shading conditions to prove the system consistency and reliability. The output results are shown in Table III. P_M refers to the arithmetic mean value of the maximum ($P_{M\text{MAX}}$) and ($P_{M\text{MIN}}$) minimum measured power values among all 100 tests. The tracking power efficiency (P_{EE}), which is used to evaluate the results, is the portion of this arithmetic mean value and actual global maximum power value tracked by the proposed algorithm under partial shading conditions ($P_{\text{EE}} = (P_M/P_A) \times 100$).

In Table IV, the performance of the proposed method is evaluated against four other established MPPT methods reported in the literature. Compared with a conventional method, such as incremental conductance [43] and the fuzzy-logic-based MPPT technique [44], the proposed method has higher efficiency and lower steady-state oscillation. Furthermore, the applied method is purely system-independent and has the capability to track GMPP under any environmental conditions. In the FLC-based MPPT method [44], the computational cost of the system is high because of the design of the different steps of the method, such as the fuzzification rule base and defuzzification stages. Furthermore, the FLC can be considered a system-dependent method because it requires more perception and comprehension of the PV system from the designer to design the different FLC parameters, such as rules and membership functions. By contrast, the proposed method finds the actual MPP in the output characteristic completely independent of the PV system.

In comparison with the standard PSO discussed in [26] and [27], the proposed method is accurate and reliable because it modifies the poor characteristics of PSO. The performance of standard PSO significantly depends on the random coefficients that are associated with the cognitive and social components of the method. The improper design of a random coefficient may significantly reduce the convergence speed of the algorithm or even lead the particles into the search space margins or local

TABLE IV
COMPARISON OF THE PROPOSED TECHNIQUE WITH OTHER MPPT METHODS

Evaluated parameters	InC [43]	FLC [44]	PSO [26], [27]	APPSO [31]	Proposed method (DEPSO)
Simplicity	**Simple**	**Medium**	**Moderate**	**High**	**Simple**
Efficiency	**High** (under Normal Conditions) **Very Low** (under Partial Shading Condition)	**High** (under Normal Conditions) **Very Low** (under Partial Shading Condition)	**High**	**High**	**Very High**
GMPP tracking capability	**No**	**Yes** (Under Certain Conditions)	**Yes**	**Yes**	**Yes**
Tracking speed	**High**	**Moderate**	**High**	**Moderate**	**High**
Steady state oscillation	**Yes**	**Yes**	**No**	**No**	**No**
Initial location dependency	**High**	**Moderate**	**High**	**High** (The initial locations of the particles are set)	**Low**
System dependency	**Dependent**	**Dependent**	**Independent**	**Independent**	**Independent**
Reliability	**Very Low**	**Low**	**Moderate –High** (Dependent on the random Coefficient)	**Moderate –High** (Dependent on the random coefficients and initial locations)	**Very High**

MPPs. In the proposed hybrid method, the detrimental effects of the random coefficients are reduced by using the DE algorithm in parallel with PSO. Compared with the modified versions of PSO methods used in the literature, the proposed method is simple to implement and shows robust and reliable performance. In the DPSO discussed in [33], the random coefficients of the PSO were removed to increase the convergence speed of the system. However, this approach will reduce the metaheuristic nature of the method, which is one of the main advantages of EA techniques. Therefore, the DPSO obtains low reliability and cannot guarantee the tracking of the actual MPP under all partial shading conditions. All three initial locations of the particles are allocated and set in the DPSO, whereas the initial location of the system is randomly set in the proposed method. According to the stochastic nature of solar irradiance, the approximate location of the MPP is not feasible and a reliable MPPT method must be capable of finding GMPP with no information about the output characteristics of the PV system. Therefore, setting the initial location for the particle may diminish the functionality of the MPPT technique under some partial shading conditions. Compared with another modified PSO-based method called APPSO, the DEPSO method has a simple implementation procedure and is independent from initial particle locations [31]. In the APPSO method, the processing time and computational burden of the system increase because all agents need to scan their own range of search space and because of the additional dimensional search space in the algorithm.

VI. CONCLUSION

This study aimed to develop a reliable and system-independent technique to track the MPP of PV system under partial shading conditions. A hybrid method called DEPSO, a combination of PSO and DE, is employed to track the actual MPP in the output of the PV system. A sequential procedure of mathematical modeling is applied to model and simulate the behavior of the PV system under partial shading conditions. The proposed MPPT method is verified through simulation and experiment under three partial shading conditions. These predefined conditions are designed to verify the reliability, speed, and accuracy of the system. The proposed DEPSO technique distinguishes the GMPP from local MPPs during mismatching conditions. The main advantages of the proposed technique are described as follows. 1) The stochastic nature of the DEPSO algorithm makes for a purely system-independent MPPT technique. 2) The presence of random numbers helps the algorithm keep its metaheuristic approach and find the GMPP in any partial shading condition. 3) The logical stoppage condition guarantees the reliability of the system to find the actual GMPP in a reasonably short time. 4) The computational burden of the algorithm is reduced, and the technique is easily implemented in a low-cost microcontroller.

REFERENCES

[1] S. Mekhilef, R. Saidur, and A. Safari, "A review on solar energy use in industries," *Renew. Sustain. Energy Rev.*, vol. 15, pp. 1777–1790, 2011.
[2] V. Salas, E. Olias, A. Barrado, and A. Lazaro, "Review of the maximum power point tracking algorithms for stand-alone photovoltaic systems," *Sol. Energy Mater. Sol. Cells*, vol. 90, pp. 1555–1578, 2006.
[3] S. K. Kollimalla and M. K. Mishra, "Variable perturbation size adaptive P&O MPPT algorithm for sudden changes in irradiance," *IEEE Trans. Sustain. Energy*, vol. 5, no. 3, pp. 718–728, Jul. 2014.
[4] T. Kok Soon and S. Mekhilef, "Modified incremental conductance algorithm for photovoltaic system under partial shading conditions and load variation," *IEEE Trans. Ind. Electron.*, vol. 61, no. 10, pp. 5384–5392, Oct. 2014.
[5] H. Patel and V. Agarwal, "MATLAB-based modeling to study the effects of partial shading on PV array characteristics," *IEEE Trans. Energy Convers.*, vol. 23, no. 1, pp. 302–310, Mar. 2008.

[6] C. Kai, T. Shulin, C. Yuhua, and B. Libing, "An improved MPPT controller for photovoltaic system under partial shading condition," *IEEE Trans. Sustain. Energy*, vol. 5, no. 3, pp. 978–985, Jul. 2014.
[7] K. Kobayashi, I. Takano, and Y. Sawada, "A study of a two stage maximum power point tracking control of a photovoltaic system under partially shaded insolation conditions," *Sol. Energy Mater. Sol. Cells*, vol. 90, pp. 2975–2988, Nov. 23, 2006.
[8] G. Carannante, C. Fraddanno, M. Pagano, and L. Piegari, "Experimental performance of MPPT algorithm for photovoltaic sources subject to inhomogeneous insolation," *IEEE Trans. Ind. Electron.*, vol. 56, no. 11, pp. 4374–4380, Nov. 2009.
[9] N. A. Ahmed and M. Miyatake, "A novel maximum power point tracking for photovoltaic applications under partially shaded insolation conditions," *Elect. Power Syst. Res.*, vol. 78, pp. 777–784, May 2008.
[10] M. Miyatake *et al.*, "Control characteristics of a fibonacci-search-based maximum power point tracker when a photovoltaic array is partially shaded," in *Proc. 4th Int. Power Electron. Motion Control Conf. (IPEMC'04)*, 2004, vol. 2, pp. 816–821.
[11] H. Patel and V. Agarwal, "Maximum power point tracking scheme for pv systems operating under partially shaded conditions," *IEEE Trans. Ind. Electron.*, vol. 55, no. 4, pp. 1689–1698, Apr. 2008.
[12] L. Peng, L. Yaoyu, and J. E. Seem, "Sequential ESC-based global MPPT control for photovoltaic array with variable shading," *IEEE Trans. Sustain. Energy*, vol. 2, no. 3, pp. 348–358, Jul. 2011.
[13] X. Weidong and W. G. Dunford, "A modified adaptive hill climbing MPPT method for photovoltaic power systems," in *Proc. IEEE 35th Annu. Power Electron. Spec. Conf. (PESC'04)*, 2004, vol. 3, pp. 1957–1963.
[14] A. M. Bazzi and S. H. Karaki, "Simulation of a new maximum power point tracking technique for multiple photovoltaic arrays," in *Proc. IEEE Int. Conf. Electro/Inf. Technol. (EIT'08)*, 2008, pp. 175–178.
[15] G. Lijun, R. A. Dougal, S. Liu, and A. P. Iotova, "Parallel-connected solar PV system to address partial and rapidly fluctuating shadow conditions," *IEEE Trans. Ind. Electron.*, vol. 56, no. 5, pp. 1548–1556, May 2009.
[16] N. Femia, G. Lisi, G. Petrone, G. Spagnuolo, and M. Vitelli, "Distributed maximum power point tracking of photovoltaic arrays: Novel approach and system analysis," *IEEE Trans. Ind. Electron.*, vol. 55, no. 7, pp. 2610–2621, Jul. 2008.
[17] N. Tat Luat and L. Kay-Soon, "A global maximum power point tracking scheme employing DIRECT search algorithm for photovoltaic systems," *IEEE Trans. Ind. Electron.*, vol. 57, no. 10, pp. 3456–3467, Oct. 2010.
[18] H. Guan-Chyun, I. H. Hung, T. Cheng-Yuan, and W. Chi-Hao, "Photovoltaic power-increment-aided incremental-conductance MPPT with two-phased tracking," *IEEE Trans. Power Electron.*, vol. 28, no. 6, pp. 2895–2911, Jun. 2013.
[19] A. I. Bratcu, I. Munteanu, S. Bacha, D. Picault, and B. Raison, "Cascaded DC–DC converter photovoltaic systems: Power optimization issues," *IEEE Trans. Ind. Electron.*, vol. 58, no. 2, pp. 403–411, Feb. 2011.
[20] J. Young-Hyok *et al.*, "A real maximum power point tracking method for mismatching compensation in PV array under partially shaded conditions," *IEEE Trans. Power Electron.*, vol. 26, no. 4, pp. 1001–1009, Apr. 2011.
[21] K. Kobayashi, I. Takano, and Y. Sawada, "A study on a two stage maximum power point tracking control of a photovoltaic system under partially shaded insolation conditions," in *Proc. IEEE Power Eng. Soc. Gen. Meeting*, 2003, vol. 4, p. 2617.
[22] C. Cecati, F. Ciancetta, and P. Siano, "A multilevel inverter for photovoltaic systems with fuzzy logic control," *IEEE Trans. Ind. Electron.*, vol. 57, no. 12, pp. 4115–4125, Dec. 2010.
[23] B. N. Alajmi, K. H. Ahmed, S. J. Finney, and B. W. Williams, "Fuzzy-logic-control approach of a modified hill-climbing method for maximum power point in microgrid standalone photovoltaic system," *IEEE Trans. Power Electron.*, vol. 26, no. 4, pp. 1022–1030, Apr. 2011.
[24] Syafaruddin, E. Karatepe, and T. Hiyama, "Artificial neural network-polar coordinated fuzzy controller based maximum power point tracking control under partially shaded conditions," *IET Renew. Power Gener.*, vol. 3, no. 2, pp. 239–253, Jun. 2009.
[25] B. N. Alajmi, K. H. Ahmed, S. J. Finney, and B. W. Williams, "A maximum power point tracking technique for partially shaded photovoltaic systems in microgrids," *IEEE Trans. Ind. Electron.*, vol. 60, no. 4, pp. 1596–1606, Apr. 2013.
[26] M. Miyatake, M. Veerachary, F. Toriumi, N. Fujii, and H. Ko, "Maximum power point tracking of multiple photovoltaic arrays: A PSO approach," *IEEE Trans. Aerosp. Electron. Syst.*, vol. 47, no. 1, pp. 367–380, Jan. 2011.
[27] L. Yi-Hwa, H. Shyh-Ching, H. Jia-Wei, and L. Wen-Cheng, "A particle swarm optimization-based maximum power point tracking algorithm for PV systems operating under partially shaded conditions," *IEEE Trans. Energy Convers.*, vol. 27, no. 4, pp. 1027–1035, Dec. 2012.
[28] V. Phimmasone, T. Endo, Y. Kondo, and M. Miyatake, "Improvement of the maximum power point tracker for photovoltaic generators with particle swarm optimization technique by adding repulsive force among agents," in *Proc. Int. Conf. Electr. Mach. Syst. (ICEMS'09)*, 2009, pp. 1–6.
[29] M. Seyedmahmoudian, S. Mekhilef, R. Rahmani, R. Yusof, and A. Asghar Shojaei, "Maximum power point tracking of partial shaded photovoltaic array using an evolutionary algorithm: A particle swarm optimization technique," *J. Renew. Sustain. Energy*, vol. 6, pp. 1–13, Mar. 2014.
[30] B. Kaewkamnerdpong and P. J. Bentley, "Perceptive particle swarm optimisation: An investigation," in *Proc. IEEE Swarm Intell. Symp. (SIS'05)*, 2005, pp. 169–176.
[31] S. Roy Chowdhury and H. Saha, "Maximum power point tracking of partially shaded solar photovoltaic arrays," *Sol. Energy Mater. Sol. Cells*, vol. 94, pp. 1441–1447, 2010.
[32] K. Ishaque, Z. Salam, M. Amjad, and S. Mekhilef, "An improved particle swarm optimization (PSO)–based MPPT for PV with reduced steady-state oscillation," *IEEE Trans. Power Electron.*, vol. 27, no. 8, pp. 3627–3638, Aug. 2012.
[33] K. Ishaque and Z. Salam, "A deterministic particle swarm optimization maximum power point tracker for photovoltaic system under partial shading condition," *IEEE Trans. Ind. Electron.*, vol. 60, no. 8, pp. 3195–3206, Aug. 2013.
[34] K. L. Lian, J. H. Jhang, and I. S. Tian, "A maximum power point tracking method based on perturb-and-observe combined with particle swarm optimization," *IEEE J. Photovoltaics*, vol. 4, no. 2, pp. 626–633, Mar. 2014.
[35] Y. J. Wang and P. C. Hsu, "Analytical modelling of partial shading and different orientation of photovoltaic modules," *IET Renew. Power Gener.*, vol. 4, no. 3, pp. 272–282, May 2010.
[36] M. Seyedmahmoudian, S. Mekhilef, R. Rahmani, R. Yusof, and E. T. Renani, "Analytical modeling of partially shaded photovoltaic systems," *Energies*, vol. 6, pp. 128–144, 2013.
[37] J. H. Seo *et al.*, "Multimodal function optimization based on particle swarm optimization," *IEEE Trans. Magn.*, vol. 42, no. 4, pp. 1095–1098, Apr. 2006.
[38] K. V. Price, R. M. Storn, and J. A. Lampinen, *Differential Evolution: A Practical Approach to Global Optimization*. Berlin, Germany: Springer-Verlag, 2005.
[39] H. Zhi-Feng, G. Guang-Han, and H. Han, "A particle swarm optimization algorithm with differential evolution," in *Proc. Int. Conf. Mach. Learn. Cybern.*, 2007, pp. 1031–1035.
[40] R. Storn and K. Price, "Differential evolution–A simple and efficient heuristic for global optimization over continuous spaces," *J. Global Optim.*, vol. 11, pp. 341–359, 1997.
[41] Z. Wen-Jun and X. Xiao-Feng, "DEPSO: Hybrid particle swarm with differential evolution operator," in *Proc. Int. Conf. Syst. Man Cybern.*, 2003, vol. 4, pp. 3816–3821.
[42] X. Rui, X. Jie, and D. C. Wunsch, "A comparison study of validity indices on swarm-intelligence-based clustering," *IEEE Trans. Syst. Man Cybern. B*, vol. 42, no. 4, pp. 1243–1256, Aug. 2012.
[43] A. Safari and S. Mekhilef, "Simulation and hardware implementation of incremental conductance MPPT with direct control method using cuk converter," *IEEE Trans. Ind. Electron.*, vol. 58, no. 4, pp. 1154–1161, Apr. 2011.
[44] M. M. Algazar, H. Al-monier, H. A. El-halim, and M. E. E. K. Salem, "Maximum power point tracking using fuzzy logic control," *Int. J. Elect. Power Energy Syst.*, vol. 39, pp. 21–28, Jul. 2012.

Mohammadmehdi Seyedmahmoudian (M'11) received the B.Sc. degree in electrical engineering from Islamic Azad University (IAU), Esfahan, Iran, in 2009, and the M. Eng. degree in industrial control and electronic (Hons.) from the University of Malaya, Kuala Lumpur, Malaysia. He is currently pursuing the Ph.D. degree in electrical engineering at the School of Engineering, Faculty of Science, Engineering and Built Environment, Geelong, Australia.

From 2012 to 2013, he was a Research Assistant with the Department of Electrical Engineering, University of Malaya. His research interests include photovoltaic systems, micro grid systems, and the artificial intelligence applications in control and optimization.

Rasoul Rahmani (M'11) received the B.Sc. degree in electrical power engineering from the University of Mazandaran (Babol Institute of Technology), Mazandaran, Iran, in 2008, and the M.Eng. degree (Hons.) from the Universiti Teknologi Malaysia, Johor, Malaysia, in 2011.

Since 2011, he has been a Research Officer with the Centre for Artificial Intelligence and Robotics, Universiti Teknologi Malaysia. He has authored around 50 publications in international journal and proceedings. His research interests include renewable and sustainable energy, power quality, and the artificial intelligence applications in control and optimization.

Saad Mekhilef (M'01–SM'12) received the B.Eng. degree in electrical engineering from the University of Setif, Setif, Algeria, in 1995, the Master's degree in engineering science, and the Ph.D. degree in electrical engineering from the University of Malaya, Kuala Lumpur, Malaysia, in 1998 and 2003, respectively.

He is currently a Professor with the Power Electronics and Renewable Energy Research Laboratory (PEARL), Department of Electrical Engineering, University of Malaya. He has authored or coauthored more than 200 publications in international journals and proceedings. He is actively involved in industrial consultancy for major corporations on power electronics projects. His research interests include power conversion techniques, control of power converters, renewable energy, and energy efficiency.

Amanullah Maung Than Oo received the B.Eng. (Hons.) degree in engineering from the International Islamic University Malaysia (IIUM), Kuala Lumpur, Malaysia, the M.Eng. degree in engineering from Melbourne University, Melbourne, Australia, in 2004, and the Ph.D. degree in electrical engineering from Victoria University, Melbourne, Australia, in 2008.

He is an Associate Professor in electrical engineering. His research interests include renewable energy, smart grid, and power systems. He has been invited to deliver key note addresses and presentations in a number of national and international workshops and conferences. He has more than 160 peer reviewed conferences and journals publications. He has supervised more than 25 Ph.D. students in power systems, renewable energy systems, and its enabling technologies.

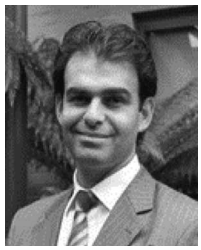

Alex Stojcevski received the Bachelor's degree in electrical engineering, the Master's degrees in education and in project-based learning (PBL) in engineering and science, the Master's degree in electrical and electronics engineering, and the Ph.D. degree from Aalborg University, Aalborg, Denmark.

He is the Deputy Head of School and the Head of Electrical and Electronics Engineering with the School of Engineering, Deakin University, Melbourne, Australia. He has held numerous senior positions across four universities and two continents. He has authored more than 150 book chapters, journals, and conference articles, and has given a number of internationally invited speaker presentations. His research interests include renewable energy and microgrid design.

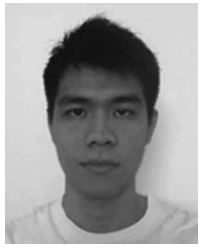

Tey Kok Soon received the B.Eng. degree (Hons.) in electrical engineering from the University of Malaya, Kuala Lumpur, Malaysia, in 2011, where he is currently pursuing the Ph.D. degree in electrical engineering.

Since 2011, he has been a Research Assistant with the Power Electronics and Renewable Energy Research Laboratory (PEARL), University of Malaya. His research interests include control of converters for solar energy, power efficiency of photovoltaic (PV) systems, and inverter control of PV systems.

Alireza Safdari Ghandhari is currently pursuing the Bachelor's degree in electrical and electronics at the University of Malaya, Kuala Lumpur, Malaysia.

He has been involved with microcontrollers, programming and robotics since he was in high school. As soon as he joined University of Malaya in 2011, he has been accepted and remained as a Researcher at the Center of Research in Applied Electronics (CRAE), University of Malaya directed by Prof. Dr. Mahmoud Moghavvemi. Under his supervision and collaboration with other members in CRAE, Alireza has two patents and won silver medal in International Conference and Exposition PECIPTA 2013.